Generalized Multi-Lag Estimators (GMLE) for Polarimetric Weather Radar Observations

David Warde, *Senior Member, IEEE,* David Schvartzman, *Senior Member, IEEE,* and Christopher D. Curtis

Abstract

Observations of weather phenomenon by polarimetric pulsed-Doppler weather radars are employed worldwide to monitor impending severe storms, flash-floods, and other weather related public hazards. The basis for processing received meteorological signals from pulsed-radar waveforms relies on stochastic processes where the accurate estimation of radar variables from received signals in additive white noise is essential for meaningful interpretation of weather phenomena and algorithm-derived products. For polarimetric weather radars, these estimates are calculated from signal correlations in time and across the horizontal and vertical polarization channels. Conventional estimators only use 1 or 2 signal correlation time-lags and may not utilize all the available information intrinsic in the received signals. Weather-variable estimates could benefit from the use of all intrinsic characteristics in the received data; accordingly, more complex estimators use multiple lags to extract additional information. However, not all estimates are improved by the use of more lags; in fact, improvement in estimates depends on signal characteristics and requires that the additional correlation lags provide new information. In this article, we derive and examine general multi-lag estimators for reflectivity, differential reflectivity, polarimetric cross-correlation coefficient, and Doppler spectrum width. We compare the performance of these proposed estimators against conventional estimators using Monte-Carlo simulations on different meteorological signal characteristics to find estimators that can improve the quality of certain radar-variable estimates.

Index Terms

weather radar, dual-polarization, generalized estimator, digital signal processing.

D. Warde is with the Cooperative Institute for Severe and High-Impact Weather Research and Operations, The University of Oklahoma, and NOAA/OAR/National Severe Storms Laboratory, Norman, OK 73072 USA (corresponding e-mail: David.A.Warde@noaa.gov).

D. Schvartzman is with the School of Meteorology and the Advanced Radar Research Center at The University of Oklahoma, Norman, OK 73069 USA.

C. Curtis is with the Cooperative Institute for Severe and High-Impact Weather Research and Operations, The University of Oklahoma, and NOAA/OAR/National Severe Storms Laboratory, Norman, OK 73072 USA.

Generalized Multi-Lag Estimators (GMLE) for Polarimetric Weather Radar Observations

I. Introduction

The Weather Surveillance Radar – 1988 Doppler (WSR-88D) radars is constantly undergoing improvements to maintain its viability and relevance to better support National Weather Service (NWS), Federal Aviation Administration (FAA), and Department of Defense (DoD) Air Force forecast and warning missions. The last major milestones in the NEXRAD program included the dual-polarization upgrade completed in June 2013 [1]. It enhanced the observing capabilities of the radar and provided a set of new radar variables that have proven to be of significant help in the interpretation of weather data in support of the NWS mission [2]. The polarimetric variables provide critical information regarding shape and nature of the hydrometeors. This information not only enhances human interpretation and understanding of weather phenomena, but it allows for the development of automatic algorithms that produce products supporting the NWS forecasters [3].

In the late 1960s through the 1980s, prior to the transition of the NEXRAD network of weather radars from the WSR-57 to the WSR-88D, researchers began investigating the use of time domain estimators (often referred to as pulse-pair or covariance estimators) (e.g., [4–8]) to replace the classical spectral moment estimators (see [8, 9] for a review of classical estimators) to obtain Doppler moment (mean velocity and spectrum width) information. From a practical side, the time domain estimators provide a lower computational load with superior quality over the classical spectral moment estimators [5]. Most of the early estimators utilized two lags of the autocorrelation; however, researchers [10, 11] realized that incorporating higher lags into the estimators improved estimates at lower signal-to-noise (SNR). In principle, optimum estimates require estimates at all lags of the autocorrelation [12]; however, depending on signal statistics, a few lags may provide optimal estimates [8].

Renewed research interest in estimators for spectral moments and polarimetric-variables – differential reflectivity (Z_{DR}), differential phase (ϕ_{DP}), and cross-correlation coefficient (ρ_{hv}) – was stimulated by dual-channel weather radars; however, since the dual-polarization upgrade on the WSR-88D network, little improvement in spectral-moment and polarimetric-variable estimators has been implemented for operational use. Researchers suggested new estimators [13–16] that may reduce the bias and standard deviation of estimates at low SNR. For example, the lag-1 Z_{DR} estimator proposed by Melnikov and Zrnić [13] is free from the influence of noise and are therefore more robust at lower SNRs. More recently, [17] proposed Generalized Multi-Lag Estimators (GMLE) that consolidate previous estimators and suggests new estimators for spectral-moment and polarimetric-variable estimates. In this generalized approach, GMLE not only utilize estimates from higher autocorrelation lags (to reduce the influence of noise), but can also include the lag-0 autocorrelation and cross-correlation estimates. Unlike previous research efforts which assume that noise contamination in the zeroth lag of the autocorrelation function can bias estimates, this work does not. When the lag-0 autocorrelation is used, GMLE relies on a sufficiently accurate noise estimation technique (e.g., [18]) to remove the noise from the zeroth-lag signal and uses this essential information, along with higher-lag correlation estimates, to improve the accuracy and precision of radar-variable estimates.

The development of the multi-lag estimators assumes a Gaussian distribution of weather radar returns. The model enables closed-form solutions and eases computational complexity permitting the extraction of copious amounts of time-critical weather information. As reported by Janssen and van der Speck [19], weather radar returns fit the Gaussian model to a high degree (75%). A more recent study [20] used the same analysis as [19] to locate tornado spectral signatures in a tornadic supercell event and found similar results (70% Gaussian like). However, they did observe spectra with dual peaks, flat tops, and wide skirts presumably from wind shear. In a follow-on study, Yu et al. [21] suggested six moments of a dual-Gaussian model better represented those observed non-Gaussian spectra. Modern weather radar signal processing successfully uses a bi-Gaussian spectrum model to recover weather signals contaminated by ground clutter [22–26]. Such clutter mitigation techniques require a piori knowledge of one of the Gaussian spectra (i.e, ground clutter has near-zero velocity) to recover the weather signal statistics. No operational signal processing technique has been developed to separate multimodal weather signal statistics, although higher order statistics and spectral flatness have been successfully used in identifying tornadic spectral signatures [27]. Clearly, such an undertaking would benefit the weather radar community, but this task is beyond the scope of this work. Instead, we concentrate on the estimates from the bulk of weather signals that have unimodal Gaussian spectra.

The formulation of the GMLE is done in a similar manner as in [14] but with the expanded meaning of "multi-lag" to include previous work with "pulse-pair" or "covariance" estimators. This framework will allow us to examine a large space of spectral-moment and polarimetric-variable estimators for possible inclusion in updates to the WSR-88D estimators. It is well know that these estimators are dependent on the signal statistics [8, 28]. For uncorrelated signals (i.e., signals with wide spectrum width compared to the Nyquist velocity), all the signal information is contained within the first couple of autocorrelation lags; however, as the signal becomes correlated within the sample space more information is conveyed at higher autocorrelation lags. Because of this behavior, researchers have proposed combining these estimators to create hybrid estimators with the optimal characteristics from the individual estimators [17, 29]. Although this will be our end goal, we will leave that effort for future work. For now, we want to know if there are any other estimators worth using in a hybrid approach.

For polarimetric weather radars, the expected autocorrelation ($R_{h,v}$) and cross-correlation (C_{hv}) functions (hereafter ACF and CCF, respectfully) of received weather returns have Gaussian power spectral densities [30, 31],

$$\begin{aligned} R_{h,v}\left(mT\right) = & \\ & S_{h,v}\rho_{h,v}\left(mT\right)\exp\left(-\frac{j\pi m\bar{v}}{v_a}\right) + N_{h,v}\delta_{m,0} \end{aligned} \tag{1}$$

$$\begin{aligned} C_{hv}\left(mT\right) = & \\ & \sqrt{S_h S_v}\rho_{hv}\rho_{h,v}\left(mT\right)\exp\left(-\frac{j\pi m\bar{v}}{v_a} + j\phi_{dp}\right) \end{aligned} \tag{2}$$

where m is the lag, T is the pulse repetition time, S is the signal power, $\rho_{h,v}$ is the correlation coefficient (equal to 1 for m = 0 and reducing as m increases) of the respective polarization channel (subscript h for horizontal or v for vertical) or cross-channel (subscript hv), $j = \sqrt{-1}$, $\overline{v}$ is the mean radial velocity, v_a the Nyquist velocity, N the system noise power, δ is the Kronecker delta (1 when m = 0 and 0 otherwise), and ϕ_{DP} is the differential phase. From (1) and (2), estimates of meteorological parameters such as reflectivity (Z_{h}), radial velocity (v_{r}), spectrum width (σ_{v}), differential reflectivity Z_{DR}, differential phase (ϕ_{DP}), and cross-correlation coefficient (ρ_{hv}) can be extracted. For example on the WSR-88D (which uses the simultaneous transmit and receive mode), the typical estimators of power (uncalibrated reflectivity, herein referred to simply as reflectivity), velocity, spectrum width, differential reflectivity, differential phase, and cross-correlation coefficient can be extracted from (1) and (2) as:

$$\hat{S}_{h,v} = \hat{R}_{h,v}(0) - \hat{N}_{h,v}, \tag{3}$$

$$\hat{Z}_{h,v} = 10\log_{10}\left(\hat{S}_{h,v}\right) \tag{4}$$

$$\hat{v}_r = \frac{v_a}{\pi}\arg\left[\hat{R}_h(T)\right], \tag{5}$$

$$\hat{\sigma}_v = \frac{v_a\sqrt{2}}{\pi}\ln\left[\frac{\hat{S}_h}{\hat{R}_h(T)}\right]^{1/2}, \tag{6}$$

$$\hat{Z}_{\mathrm{DR}} = 10\log_{10}\left(\frac{\hat{S}_h}{\hat{S}_v}\right) \tag{7}$$

$$\phi_{dp} = \arg\left[C_{hv}(0)\right],\ \text{and} \tag{8}$$

$$\rho_{hv} = \frac{|C_{hv}(0)|}{\sqrt{\hat{S}_h\hat{S}_v}}, \text{for } m = \{0,1\}. \tag{9}$$

The v_{r} in (5) and ϕ_{DP} in (8) use the arguments of the ACF and CCF respectively and multi-lag estimates require unwrapping the phases of the higher lags as suggested by ([14, 28, 32]). For our purposes, it can be seen that the estimators for Z_{h}, σ_{v}, Z_{DR}, and ρ_{hv} in (4), (6), (7), and (9) use the magnitude of the ACF. To use the lag-0 autocorrelation an accurate estimate of system noise power, $\hat{N}_{h,v}$ is needed. Thus, when system noise power is inaccurately measured or unavailable, higher-lag estimators, $m > 0$ in (1), that do not require noise estimates can be used (e.g., [13] and many others). In addition, and to further reduce uncertainty in the estimates, multi-lag estimators have been suggested [14]. In systems like the WSR-88D that provide valid system noise estimates [18], no multi-lag estimators have been suggested that include the use of the lag-0 estimates. Thus, we generalized the least-square estimators based on the fit of a Gaussian model to include lag-0 autocorrelation and cross-correlation estimates and improve multi-lag estimators of the spectral-moment and polarimetric variables [17].

In this article, we introduce the GMLE for Z_{h}, Z_{DR}, ρ_{hv}, and σ_{v}. We derive the GMLE for all lag estimators and provide closed form solutions for the lag-0 estimators in section II. We assess the performance with simulations of the derived lag-0 estimators for lags up to lag-3 of the ACF and CCF in section III. Finally, section IV summarizes our findings and future plans.

II. The Generalized Multi-Lag Estimators (GMLE)

Parameters for multi-lag radar-variable estimators based on linear least-squares estimators of the autocorrelation or cross-correlation can be realized by minimizing the residuals of the squared distance between the expected and the observed autocorrelation or cross-correlation values. For the autocorrelation function, a Gaussian-shaped function can be expected [30] (Eq. 6.5):

$$\rho\left(mT\right) = \exp\left[-8(\pi\sigma_v mT/\lambda)^2\right] \tag{10}$$

The natural log of a Gaussian function is a parabolic function, which we can use to simplify the fitting process. Thus, the first step toward a generalized least squares Gaussian fit for higher lags is to take the natural log of autocorrelation:

$$y_m = \ln\left[\left|R_{h,v}\left(mT\right) - N_{h,v}\delta_{m,0}\right|\right] = am^2T^2 + b - ak^2T^2 \tag{11}$$

where $a = -8(\pi\sigma_{\mathrm{v}}\ /\lambda)^2$, $b = \ln[\rho\left(kT\right)S_{h,v}]$, and k is the lag-number of the correlation coefficient of interest, which form the merit function:

$$F(a,b) = \sum_{m\in X}\left[a\left(m^2 - k^2\right)T^2 + b - \hat{y}_m\right]^2 \tag{12}$$

where $X \subset \mathbb{N}_0$ and $\mathbb{N}_0$ is the set of nonnegative integers $\{0,\ 1,\ 2,\ \ldots\}$. The sum of the residuals is minimized when the derivatives with respect to each parameter, a and b are zero. We define a similar relationship for the cross-correlation function and solve for c and d over the subset W of all integers $\mathbb{Z}$,

$$z_n = \ln\left[\left|C_{hv}\left(nT\right)\right|\right] = cn^2T^2 + d - ck^2T^2 \tag{13}$$

where $c = -8(\pi\sigma_{\mathrm{v}}\ /\lambda)^2$ and $d = \ln[\rho\left(kT\right)S_{\mathrm{hv}}\rho_{\mathrm{hv}}]$, $S_{hv} = \sqrt{S_hS_v}$, and k is the lag-number of the correlation coefficient of interest and form the merit function:

$$G(c,d) = \sum_{n\in W}\left[c\left(n^2 - k^2\right)T^2 + d - \hat{z}_n\right]^2. \tag{14}$$

Solutions of a, b, c, and d in (12) and (14) lead to different estimators used in polarimetric weather radars and can be found for different subsets of m and n, and for different lags of k. Hereafter, we use the following terminology: lag-0 estimators when k = 0, lag-1 estimators when k = 1, lag-2 estimators when k = 2, etc. For example, [14] used $m = \{1, ...,$M$\}$, n = {-M,..., M} to create a set of multi-lag estimators for k = 0; whereas, [13] formed the lag-1 ρ_{hv} estimator with k = 1.

The following expressions present the GMLE for signal power, spectrum width, differential reflectivity, and cross-correlation coefficient as a function of a, b, c, and d.

$$\hat{S}_{h,v} = \exp\left(b\right)/\rho\left(kT\right) \tag{15}$$

$$\hat{\sigma}_{h,v} = \frac{\lambda\sqrt{-2a}}{4\pi} \tag{16}$$

$$\hat{Z}_{DR} = \frac{10}{\ln\left(10\right)}\left[b_h - b_v\right] \tag{17}$$

$$\hat{\rho}_{hv} = \exp\left[a - \frac{b_h + b_v}{2}\right] \tag{18}$$

Next, we derive the GMLE and provide closed-form derivations for all lag-0 estimators (i.e., $k = 0$) with sequential sets of m starting at 0 or 1.

A. Derivation Of the GMLE

1) ACF: With $X \subset \mathbb{N}_0$ and $x = |X|$ (i.e., cardinal or number of elements in X). Using the least squares fit, the merit function (12) with $m \in X$ reaches its minimum when the partial derivatives with respect to a and b are zero:

$$\begin{gathered}\frac{\partial F(a,b)}{\partial a} = 2aT^4 \sum_{m \in X} m^4 - \ldots \\ \ldots - 4ak^2T^4 \sum_{m \in X} m^2 + 2bT^2 \sum_{m \in X} m^2 - \ldots \\ \ldots - 2T^2 \sum_{m \in X} m^2 \hat{y}_m + 2xak^4T^4 - \ldots \\ \ldots - 2xbk^2T^2 + 2k^2T^2 \sum_{m \in X} \hat{y}_m = 0\end{gathered} \tag{19}$$

and

$$\begin{gathered}\frac{\partial F(a,b)}{\partial b} = 2aT^2 \sum_{m \in X} m^2 - \ldots \\ \ldots - 2xak^2T^2 + 2xb - 2 \sum_{m \in X} \hat{y}_m = 0.\end{gathered} \tag{20}$$

Solving for b in (19) and (20):

$$\begin{aligned} b &= \frac{\left(\begin{gathered}\sum_{m \in X} m^2 \hat{y}_m - aT^2 \sum_{m \in X} m^4 + \ldots \\ \ldots + 2ak^2T^2 \sum_{m \in X} m^2 - xak^4T^2 - \ldots \\ \ldots - k^2 \sum_{m \in X} \hat{y}_m\end{gathered}\right)}{\left(\sum_{m \in X} m^2 - xk^2\right)} \\ &= \frac{\sum_{m \in X} \hat{y}_m - aT^2 \sum_{m \in X} m^2 + xak^2T^2}{x}.\end{aligned} \tag{21}$$

Solving for a in (21) yields

$$a = \frac{\sum_{m \in X} m^2 \sum_{m \in X} \hat{y}_m - x \sum_{m \in X} m^2 \hat{y}_m}{T^2 \left[\left(\sum_{m \in X} m^2\right)^2 - x \sum_{m \in X} m^4\right]}. \tag{22}$$

Inserting (22) into (21) and simplifying

$$b = \frac{\left[\begin{gathered}\left(\sum_{m \in X} m^2 - xk^2\right) \sum_{m \in X} m^2 \hat{y}_m + \ldots \\ \ldots + \left(k^2 \sum_{m \in X} m^2 - \sum_{m \in X} m^4\right) \sum_{m \in X} \hat{y}_m\end{gathered}\right]}{\left(\sum_{m \in X} m^2\right)^2 - x \sum_{m \in X} m^4}. \tag{23}$$

2) CCF: Let $W \subset \mathbb{Z}$ and $w = |W|$; then, the least squares fit for the merit function for the CCF (14) with $n \in W$ reaches its minimum when the partial derivatives with respect to c and d are zero. Both c and d have similar forms as (22) and (23); however, we are only concerned with d

$$d = \frac{\begin{bmatrix} \left(\sum\limits_{n\in W} n^2 - wk^2\right)\left(\sum\limits_{n\in W} n^2 \hat{z}_n + \dots\right. \\ \left.\dots + \left(k^2 \sum\limits_{n\in W} n^2 - \sum\limits_{n\in W} n^4\right) \sum\limits_{n\in W} \hat{z}_n \right. \end{bmatrix}}{\left(\sum\limits_{n\in W} n^2\right)^2 - w \sum\limits_{m\in W} n^4} \tag{24}$$

B. Lag-0 Estimators

Closed form solutions for lag-0 estimators (i.e., $k = 0$) of (22) and (23) with sequential sets of X when the first term is 0 or 1 can be obtained with the use of Faulhaber's formula for the 2nd and 4th power sums

$$\begin{aligned} \sum_{m=0}^{M} m^2 = \sum_{m=1}^{M} m^2 &= \frac{M(M+1)(2M+1)}{6} \text{ and} \\ \sum_{m=0}^{M} m^4 = \sum_{m=1}^{M} m^4 &= \dots \\ \dots &= \frac{M(M+1)(2M+1)\left(3M^2+3M-1\right)}{30} \end{aligned} \tag{25}$$

Letting $X = \{0, 1, \dots, M\}$, $x = (M + 1)$ and inserting (25) into (22) and (23) yields

$$a = \frac{30 \sum\limits_{m=0}^{M} \left[6m^2 - M(2M+1)\right] \hat{y}_m}{T^2 M (M+1)(2M+1)(M+2)(8M-3)} \tag{26}$$

and

$$b = \frac{6 \sum\limits_{m=0}^{M} \{3M^2 + 3M - 1 - 5m^2 \quad \hat{y}_m}{(M+1)(M+2)(8M-3)}. \tag{27}$$

The estimates of a and b in (26) and (27) result when including the lag-0 ACF estimate; however, if X = {1, …, M} in the summations in (22) and (23) (i.e., excluding the lag-0 autocorrelation estimate[1]) the estimates of a and b become (28) and (29) which are the same as proposed by Lei et al. [14, eq. (5a) and (5b)]:

$$a_L = \frac{30 \sum\limits_{m=1}^{M} \left[6m^2 - (M+1)(2M+1)\right] \hat{y}_m}{T^2 M (M-1)(M+1)(2M+1)(8M+11)} \tag{28}$$

and

$$b_L = \frac{6 \sum\limits_{m=1}^{M} \left(3M^2 + 3M - 1 - 5m^2\right) \hat{y}_m}{M(M-1)(8M+11)}. \tag{29}$$

More solutions for lag-0 estimators can be obtained for a and b in (22) and (23) by deriving 2nd and 4th power sums for all terms in X (i.e., excluding missing terms as in the derivation of (28) and (29)). A summary of these lag-0 estimators for all sets of 2 or more elements in the set $\{0, 1, 2, 3\}$ (i.e., using lag-0 through lag-3 of the ACF) derived from (22) and (23) are shown in table I.

TABLE I

THE LAG-0 ESTIMATE PARAMETERS FOR 2, 3, AND 4-ELEMENT SUBSETS OF $m = \{0,\,1,\,2,\,3\}$ DERIVED FROM (12) TO CREATE ESTIMATORS IN (15), (16), (17), AND (18).

m	aT^2	b
$\{0,\,1\}$[1]	$-\hat{y}_0 + \hat{y}_1$	$\hat{y}_0$
$\{0,\,1,\,2\}$[2]	$\frac{-5\hat{y}_0-2\hat{y}_1+7\hat{y}_2}{26}$	$\frac{17\hat{y}_0+12\hat{y}_1-3\hat{y}_2}{26}$
$\{0,\,2\}$	$\frac{-\hat{y}_0+\hat{y}_2}{4}$	$\hat{y}_0$
$\{1,\,2\}$[1,3]	$\frac{-\hat{y}_1+\hat{y}_2}{3}$	$\frac{4\hat{y}_1-\hat{y}_2}{3}$
$\{0,\,1,\,2,\,3\}$	$\frac{-7\hat{y}_0-5\hat{y}_1+\hat{y}_2+11\hat{y}_3)}{98}$	$\frac{7\hat{y}_0+6\hat{y}_1+3\hat{y}_2-2\hat{y}_3}{14}$
$\{0,\,1,\,3\}$	$\frac{-10\hat{y}_0-7\hat{y}_1+17\hat{y}_3}{146}$	$\frac{41\hat{y}_0+36\hat{y}_1-4\hat{y}_3}{73}$
$\{0,\,2,\,3\}$	$\frac{-13\hat{y}_0-\hat{y}_2+14\hat{y}_3}{122}$	$\frac{97\hat{y}_0+45\hat{y}_2-20\hat{y}_3}{122}$
$\{1,\,2,\,3\}$[4]	$\frac{-11\hat{y}_1-2\hat{y}_2+13\hat{y}_3}{98}$	$\frac{6\hat{y}_1+3\hat{y}_2-2\hat{y}_3}{7}$
$\{0,\,3\}$	$\frac{-\hat{y}_0+\hat{y}_3}{9}$	$\hat{y}_0$
$\{1,\,3\}$	$\frac{-\hat{y}_1+\hat{y}_3}{8}$	$\frac{9\hat{y}_1-\hat{y}_3}{8}$
$\{2,\,3\}$	$\frac{-\hat{y}_2+\hat{y}_3}{5}$	$\frac{9\hat{y}_2-4\hat{y}_3}{5}$

[1] cf., [30].

[2] cf., [29, for σ_{v}].

[3] cf., [14, for $M = 2$].

[4] cf., [14, for $M = 3$].

Closed form solutions for lag-0 estimators of d in (24) are needed to complement those for b in (27) and (29)

[1]Excluding lag-0 reduces the number of elements x to M on right-hand side of (22) and (23),

to obtain $\hat{\rho}_{hv}$. From (25) we derive:

$$\sum_{m=-M}^{M} m^2 = \frac{M\,(M+1)\,(2M+1)}{3} \text{ and}$$
$$\sum_{m=-M}^{M} m^4 = \dots \tag{30}$$
$$\dots = \frac{M\,(M+1)\,(2M+1)\,\left(3M^2+3M-1\right)}{15}$$

Letting $W = \{-M, \dots, M\}$, $w = (2M+1)$ and inserting (30) in (24) results in (31) for d when using (27) (i.e., using lag-0 ACF) or (29) (when not using lag-0 ACF) for b to estimate lag-0 estimators of ρ_{hv} in (18).[2]

$$d = \frac{3 \sum\limits_{n=-M}^{M} \left\{ \left(3M^2+3M-1-5n^2\right) z_n \right.}{(2M-1)\,(2M+1)\,(2M+3)}. \tag{31}$$

III. Performance of the GMLE

To understand the performance of the GMLE, we need to investigate their statistical properties as a function of SNR, σ_{v}, Z_{DR}, ρ_{hv}. There are three commonly used approaches to quantify statistical biases and standard deviations [13]; 1) using the probability distributions of estimates to obtain first and second order moments, 2) using perturbation analysis [30], and 3) using signal simulations over a large number of realizations. Certain trade-offs of these approaches must be considered when deciding the most suitable for the desired analysis. For 1), although the distributions of Z_{h}, σ_{v}, Z_{DR}, and ρ_{hv} estimates are known for independent samples [33], weather signal samples are generally highly correlated (except in very wide spectrum width scenarios), this limits the usefulness of this approach for the GMLE performance evaluation. Especially since the goal is to evaluate the GMLE in a large parameter space, and considering that GMLE's are expected to outperform conventional estimators especially at narrow spectrum width (i.e., highly correlated samples). Several results regarding weather signal statistics have been obtained with 2) [30, 31], and have proven to work well in cases with a relatively large number of samples (usually the case with weather radar scans). However, given the number of lag combinations possible and the complexity of the GMLE's (eqs. 19 to 31 and Table I), using 2) would require extensive derivations (for each estimator). Nevertheless, we provide a mathematical formulation for the perturbation analysis in the Appendix, which can be used to derive theoretical bounds for the bias and standard deviation of the GMLE. Lastly, 3) has been used extensively for evaluating the performance of estimators using established time-series I/Q simulation methods [34–36]. Although this approach can be computationally expensive, it provides flexibility to simulate a wide range of signal parameters in a controlled and systematic way. Therefore, we use a Monte-Carlo simulation scheme to produce weather-like time-series I/Q simulations [35] to systematically quantify the bias and standard deviation of the proposed estimators in a large space of signal conditions (similar to [15]). For these simulations,

[2]Although not discussed here, it is easy to verify that the lag-1 $\hat{\rho}_{hv}$ [13, (9b) instead of (9a) in (10)] is obtained from (18) when $k = 1$, $X \equiv \{0, 1\}$ in (23) and $W \equiv \{-1, 0, 1\}$ in (24).

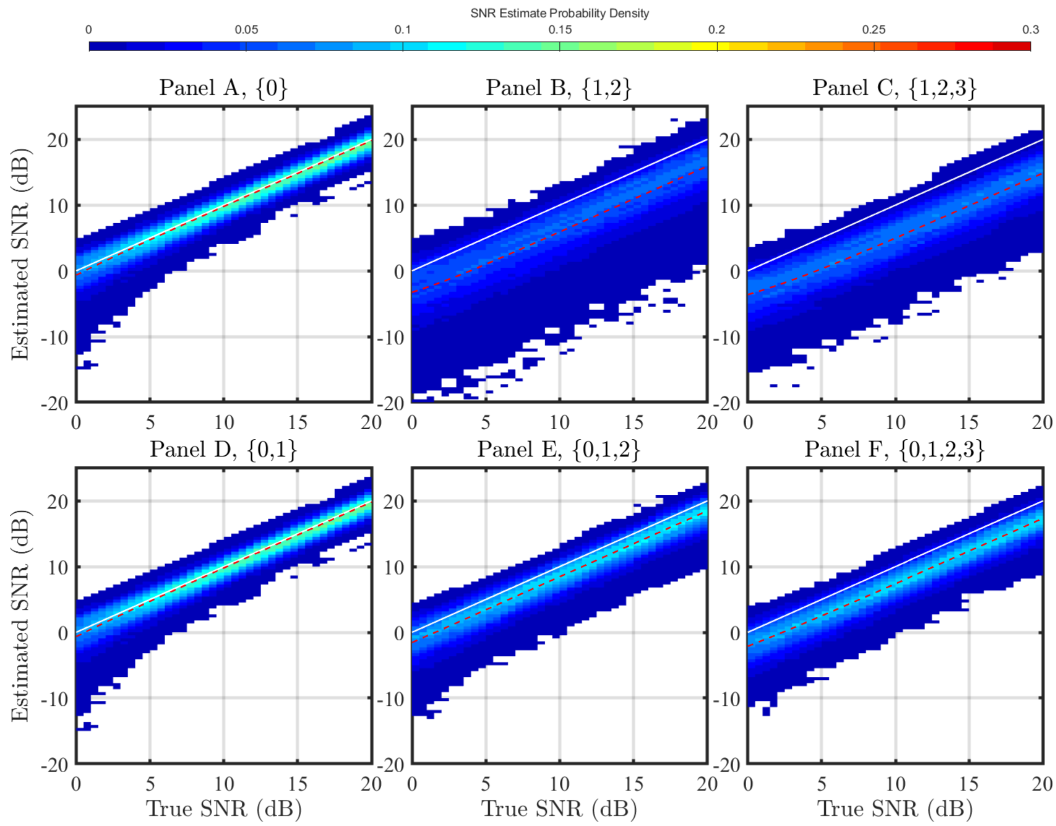

Fig. 1. Simulation results showing probability density functions of true vs. estimated SNRs for different lags were produced with 5,000 realizations and with system parameters of λ = 10.7 cm (wavelength), pulse repetition time (PRT) = 3,120 μs, dwell time = 50 ms (defined as the PRT multiplied by the number of samples), v_{r} = 0 m s^{-1}, and σ_{v} = 4 m s^{-1}. These parameters represent benchmark conditions typically used to assess the performance of estimators for the Surveillance mode (i.e., unambiguous range detection) used in the WSR-88D.

we assume a well calibrated and balanced system (i.e., all system biases are zero and the noise is the same in both channels).

Simulation results presented in Figs. 1 – 4 were produced with 5,000 realizations and with system parameters of λ = 10.7 cm (wavelength), pulse repetition time (PRT) = 3,120 μs, dwell time = 50 ms (defined as the PRT multiplied by the number of samples), and v_{r} = 0 m s^{-1}. For SNR analysis in Fig. 1, σ_{v} = 4 m s^{-1}; whereas for Z_{DR} and ρ_{hv} analysis in Figs. 2 – 3, σ_{v} = 2 m s^{-1} with SNR in the horizontal channel set to 20 dB. These parameters represent benchmark conditions typically used to assess the performance of estimators used for the Surveillance mode (i.e., unambiguous range detection) in the WSR-88D. Additionally, we show ρ_{hv} analysis for reduced benchmark conditions of SNR = 5 dB and σ_{v} = 1 m s^{-1} in Fig. 4.

Estimates of reflectivity $Z_{h,v}$ (4) is derived from the power reflected back from precipitation to the weather radar [30, 31, 37]. The ACF is used to extract the noise-free power measurement $\hat{S}_{h,v}$ (3). Since accurate noise estimates $\hat{N}_{h,v}$ have a direct impact on the accuracy of $\hat{Z}_{h,v}$, $\hat{S}_{h,v}$ have been suggested that avoid the ACF at lag-0 when noise estimation is unattainable; still, we will examine the performance of all $S_{h,v}$-estimators listed in table I. Fig. 1 shows the probability density of estimated signal-to-noise ratio [SNR, $10\log(S_{h,v}/N_{h,v})$] for each selected estimator, with m = $\{0\}$ (i.e., the conventional estimator), $\{0,1\}$, $\{1,2\}$, $\{0,1,2\}$, $\{1,2,3\}$, and $\{0,1,2,3\}$. The color scale, shown at the top, presents the probability density (ranging from 0 to 0.3) for the estimates as a function of true SNR. The red dashed line is the estimate mean of SNR from 0 to 20 dB and the white line shows unbiased SNR. The upper left panel is the conventional estimator used in most weather radar systems. This is also the solution to the $\{0,1\}$-estimator (the bottom left panel, see table I). Here, it is obvious that the other estimators are biased with those using lag-0 (panels D, E, and F) having less bias than those not using it (panels B and C). This indicates that estimators using the lag-0 autocorrelation with noise compensation have lower bias and lower variance. Although not shown, the bias and variance of the GMLE improve as the σ_{v} decreases. It would appear from our analysis and the representative images shown that one would do better by obtaining an accurate noise estimate and using the noise-compensated $\hat{S}_{h,v}$; furthermore, additional lags do not appear to improve $\hat{S}_{h,v}$.

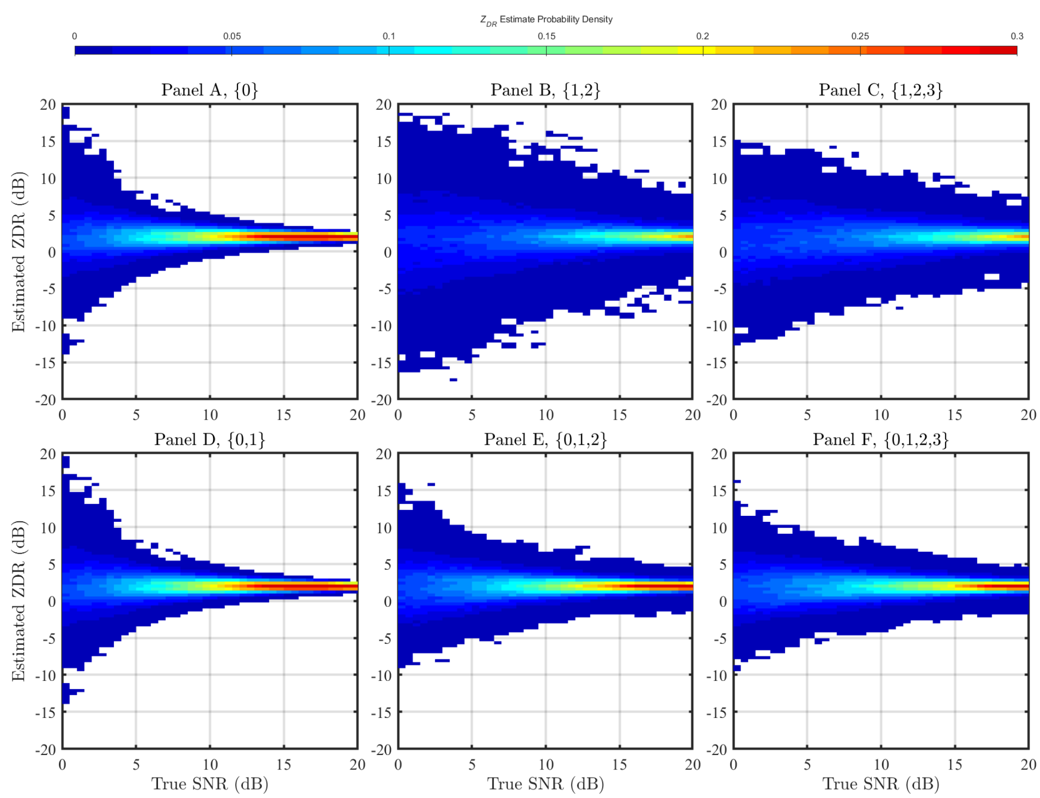

Fig. 2. Similar to Fig. 1, but for Z_{DR} estimators for different lags and with σ_{v} = 2 m s^{-1}, Z_{DR} = 2 dB, and ρ_{hv} = 0.99.

The differential reflectivity Z_{DR} is the logarithmic ratio of Z_h to Z_v (7) and helps to characterize microphysical precipitation-states [37]. From the performance of the estimators of $S_{h,v}$ shown in Fig. 1, one might suspect that $\hat{Z}_{DR}$ from higher lags and without noise compensation would be similarly biased and highly variant as those for $\hat{S}_{h,v}$. However, this is not the case as we will soon see. Fig. 2 shows the probability density of $\hat{Z}_{DR}$ for each selected estimator shown in Fig. 1. For this simulation, σ_{v} = 2 m s^{-1}, Z_{DR} = 2 dB, and ρ_{hv} = 0.99. The color scale, shown at the top, shows the probability density for the estimates (0 – 0.3) as a function of true SNR. The upper left panel is the conventional estimator used in most weather radar systems and is also the solution to the {0,1}-estimator for Z_{DR} in the bottom left panel (see table I). Unlike the estimators for $S_{h,v}$, the Z_{DR}-estimators shown are unbiased. That is, both $\hat{S}_h$ and $\hat{S}_v$ estimates are biased in a similar manner but are unbiased relative to each other. However, variance of the Z_{DR}-estimators increase as the signal decreases toward noise (i.e., toward an SNR of 0 dB). Additionally, those Z_{DR}-estimators not using the lag-0 ACF have more variance (e.g., compare panel B to panel E and panel C to panel F). Furthermore, comparing panels D – F a slight decrease in variance at low SNR for estimators using higher lags is observed with the {0,1,2,3}-estimator (panel F) having the lowest variance near 0 dB SNR. Although not shown, the variance of the estimators improves as the σ_{v} decreases; degrades as ρ_{hv} decreases; and is unaffected by Z_{DR}.

The cross-correlation coefficient ρ_{hv} (unitless) provides a measure of the consistency in both amplitude and phase between the horizontal and vertical polarization channels. Spherical particles of precipitation have values near one, while precipitation with dissimilar back scatter polarization properties (i.e., type, shape, or orientation) reduces the ρ_{hv} toward zero [38]. Useful ranges for precipitation of ρ_{hv} are between 0.8 to 1. The performance of the ρ_{hv}-estimators is important to properly characterize the precipitation. Fig. 3 shows the probability density of estimated ρ_{hv} for each selected estimator shown in Fig. 1. For this simulation, SNR = 20 dB, σ_{v} = 2 m s^{-1}, and Z_{DR} = 0 dB. The color scale, shown at the top, shows the probability density for the estimates (0 – 0.3) as a function of true ρ_{hv}. The red dashed line is the estimate mean for each ρ_{hv} from 0.8 to 1 with the white line showing unbiased ρ_{hv}. The upper left panel is the conventional estimator used in most weather radar systems and is also the solution to the {0,1}-estimator for ρ_{hv} in the bottom left panel (see table I). The ρ_{hv}-estimators are biased for estimators using lag-3, but improve as σ_{v} increases. Although not shown, the variance of the estimators improve as the σ_{v} decreases, degrades as SNR decreases; and is unaffected by Z_{DR}. Unlike the estimators for SNR and Z_{DR}, higher-lag ρ_{hv} estimators perform better for lower SNR and narrower σ_{v} than the conventional ρ_{hv} estimator. As an example, lowering the SNR to 5 dB and σ_{v} to 1 m s^{-1} shows (see Fig. 4) that variance increases for all the estimators as compared to WSR-88D benchmark using an SNR = 20 dB and σ_{v} = 2 m s^{-1} (see Fig. 3); however, the use of higher-lag ρ_{hv} estimators such as in panels E and F perform slightly better than the conventional ρ_{hv} estimator (panel A) as seen in Fig. 4.

The spectrum width σ_{v} is a measure of the distribution of radial velocities from targets within the radar resolution volume [30, 31]. It can be derived from the 2^{nd} central spectral moment, but under the assumption of a Gaussian spectrum most modern weather radars use the ACF to derive σ_{v} [8]. Here, we will show comparisons of the σ_{v}-estimators that use the ACF (see table I). Fig. 5 shows the probability density of the $\hat{\sigma}_{vn}$ ($\hat{\sigma}_v/2v_a$) for each of the selected estimators shown in table I. For the simulations in Fig. 5 – 7, 10,000 realizations were created with system parameters of λ = 10.7 cm, PRT = 986 μs, dwell time = 50 ms, velocity = 0 m s^{-1}, and SNR = 10 dB.

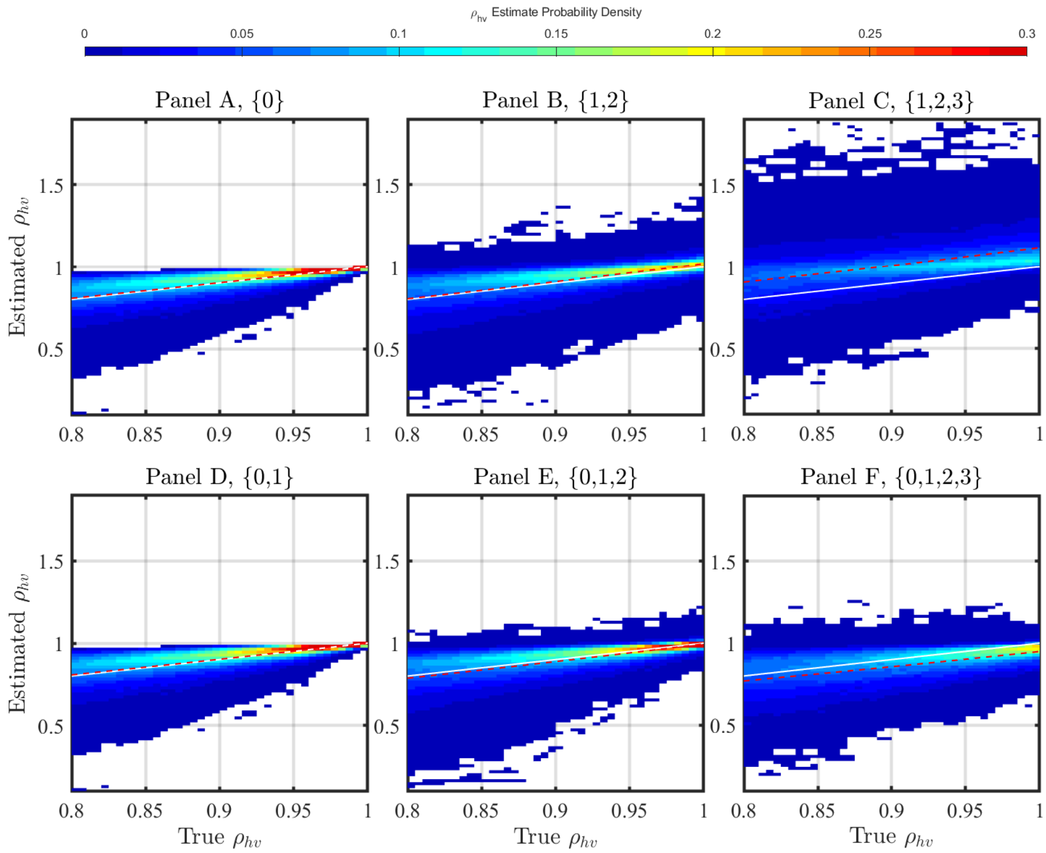

Fig. 3. Similar to Fig. 1, but for ρ_{hv} estimators, and for different lags with SNR = 20 dB and σ_{v} = 2 m s^{-1}.

These parameters represent benchmark conditions typically used to assess the performance of estimators used for the Doppler mode (i.e., extended unambiguous velocity recovery) in the WSR-88D.

The color scale, shown at the top, shows the probability density (typical values from 0 to 1) for the estimates (0 – 0.1) as a function of true σ_{v}. The white line shows unbiased σ_{vn} from 0 to 0.2. The individual σ_{v}-estimators (panels B – L) have known errors of estimates; thus, hybrid estimators exploit trade offs between the individual estimators by choosing ones that best fit the given signal characteristics to improved overall performance. In panel A, hybrid σ_{v}-estimator selects between estimators in panels B, E and G [29].The variance of the σ_{v}-estimators improve as the SNR increases; still, reduced variance of these estimators can be realized by using matched autocorrelations [39]. Warde and Torres quantified these performance improvements for the estimators shown in panels B – D [40]. Fig. 6 panels B – D show the estimators from Fig. 5 panels B – D when matched autocorrelations (MA) are incorporated. These estimators produce a meaningless value when the magnitude of the numerator is smaller than the magnitude in the denominator. Using this fact, they proposed a simple hybrid estimator [39] using the MA estimators as shown in panel A of Fig. 6. In this simple approach, the estimator that has the best wide spectrum

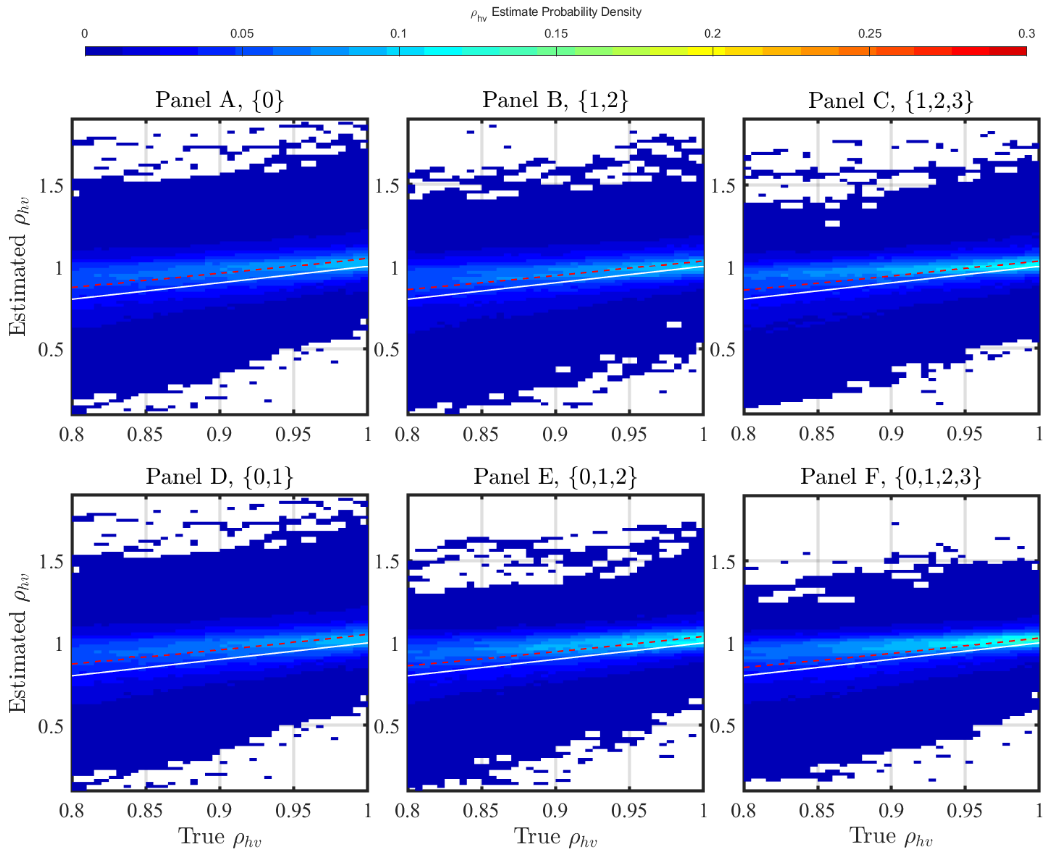

Fig. 4. Similar to 3, but for SNR = 5 dB and σ_v = 1 m s^{-1}

width performance is used, panel B, as long as it does not provide a meaningless value, which is more likely as the spectrum width becomes narrower. If a meaningless value occurs, the next best "wide" spectrum width estimator, panel C is selected. Lastly, if the estimator in panel C produces a meaningless value, the estimator from panel D is chosen. The simple hybrid σ_v estimator shows marked improvement over the hybrid σ_v estimator in Fig. 5; nevertheless, the simple hybrid estimator does not produce the lowest errors of estimates as seen by comparing the higher probability of (lighter blue) narrow spectrum width estimates in panels C and D with the lower probability of (darker blue) narrow σ_v estimates in panel A of Fig. 6. Accordingly, Warde and Schvartzman [17] suggested selecting between estimators based on the statistical characteristics of the estimators to derive lookup tables (LUTs), which are then used to determine the estimator that results in the lowest bias B and standard deviation SD of estimates under specific conditions. In their work, they proposed using a weighted mean squared error (WMSE), $(\alpha B^2 + \beta SD^2)/(\alpha + \beta)$ with $\alpha = 3$ and $\beta = 1$, to create the LUTs. Similarly, Fig. 7 shows the same MA σ_v estimators in panels B – D with the hybrid estimator using the WMSE suggested by Warde and Schvartzman [17]. Here a clear improvement in narrow σ_v is seen when comparing Fig. 6 panel A to those in Fig. 7 panel A.

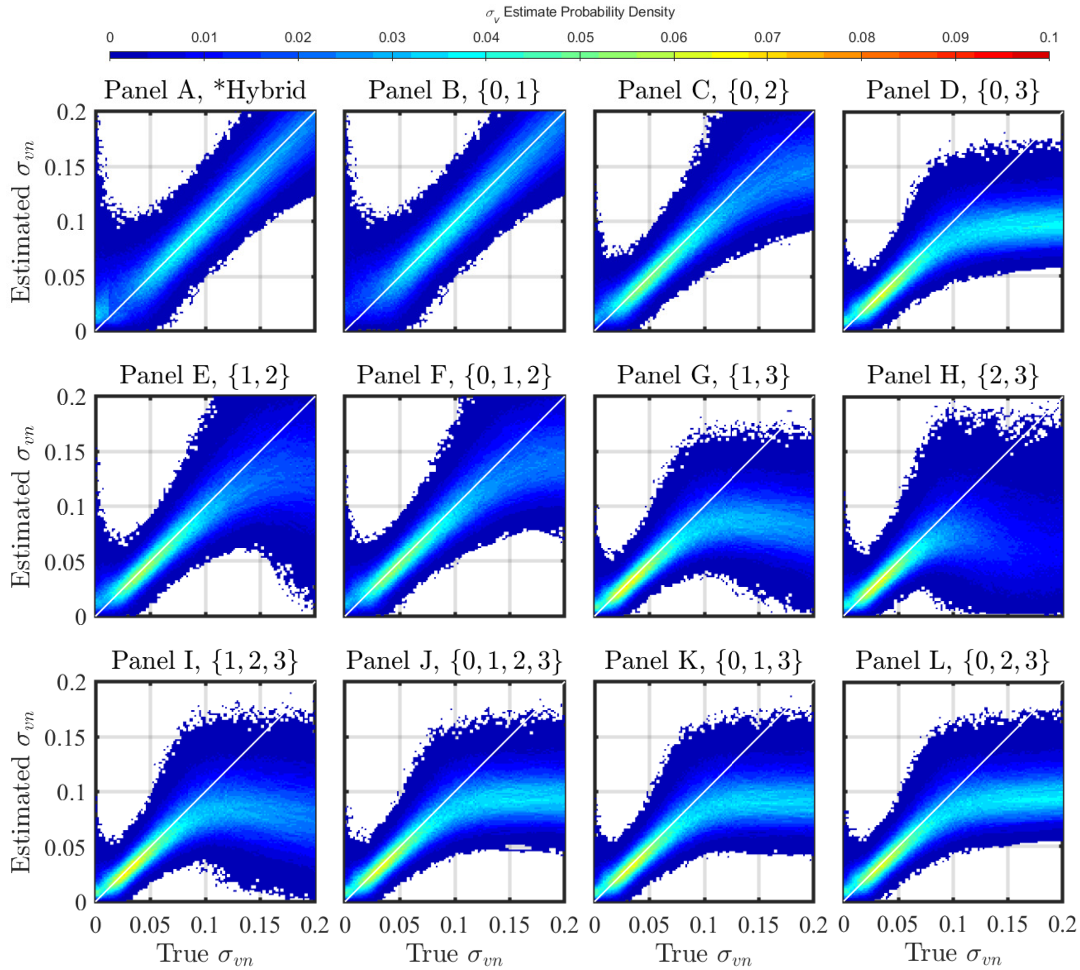

Fig. 5. Probability density functions of the $\hat{\sigma}_{vn}$ ($\hat{\sigma}_v/2v_a$) for each of the selected estimators in table I are shown in panels B – I. Panel A shows the performance of the hybrid σ_v-estimator from [29]. Here, 10,000 realizations were created with system parameters of λ = 10.7 cm, PRT = 986 μs, dwell time = 50 ms, velocity = 0 m s^{-1}, and SNR = 10 dB.

IV. Conclusion

In this work, we formulated the Generalized Multi-Lag Estimators (GMLE) for the estimates of Z_h, σ_v, Z_DR, and ρ_hv. We compared the GMLE estimators with those estimators used in modern weather radars. We showed in section II that the use of the lag-0 in the formulation of estimators improved the estimates which suggests that it would be better to obtain good noise estimates than to avoid the use the lag-0 ACF. This was most obvious in the Z_h-estimators where other estimators produced increased bias and variance of the $\hat{Z}_h$ when not using the lag-0 ACF. For the other GMLE estimators (i.e., σ_v, Z_DR, and ρ_hv), at times, the use of higher ACF and CCF lags also improved the estimates leading to some researchers creating hybrid-estimators (i.e., combining multiple estimators) to improve the overall quality of the estimates. In the future, we plan to create hybrid-GMLE estimators based on

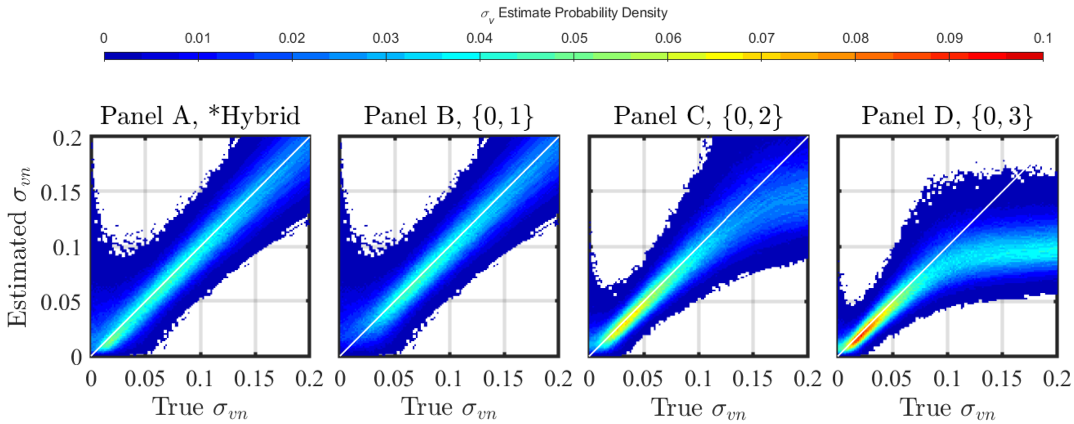

Fig. 6. Estimated probability density functions of $\hat{\sigma}_{vn}$. Panel A shows the performance of the hybrid σ_v-estimator from [39, 40], while panels B – D show the σ_v estimators when matched autocorrelations (MA) are incorporated.

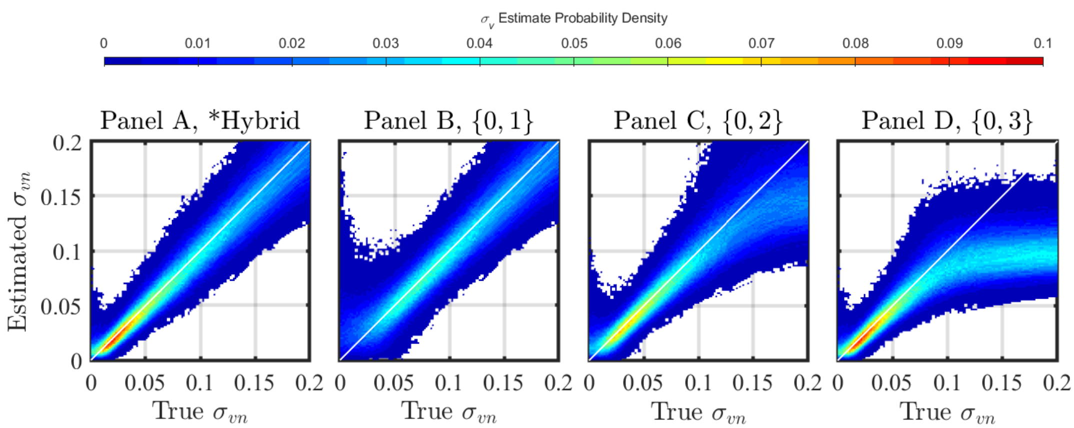

Fig. 7. Similar to 6. The MA σ_v estimators in panels B – D but combining the MA σ_v estimators with the weighted MSE estimator suggested by Warde and Schvartzman [17] for the hybrid estimator in panel A.

the results from section II.

Acknowledgment

The authors would like to thank Dr. Valery Melnikov, Dr. Guifu Zhang, and anonymous reviewers for providing comments to improve the manuscript. The computing of lookup tables with estimator-performance metrics for this project was performed at the OU Supercomputing Center for Education & Research (OSCER).

References

[1] Radar Operations Center, "NEXRAD/WSR-88D History," Radar Operations Center, White Paper, 2018, Accessed: Oct. 7, 2022. Available: https://www.roc.noaa.gov/WSR88D/PublicDocs/NEXRAD.pdf.

[2] D. S. Zrnić and A. V. Ryzhkov, "Polarimetry for weather surveillance radars," *Bulletin of the American Meteorological Society*, vol. 80, no. 3, pp. 389–406, 1999. DOI: 10.1175/1520-0477(1999)080⟨0389:PFWSR⟩2.0.CO;2.

[3] K. A. Scharfenberg *et al.*, "The Joint Polarization Experiment: Polarimetric Radar in Forecasting and Warning Decision Making," *Weather and Forecasting*, vol. 20, no. 5, pp. 775–788, 2005. DOI: 10.1175/WAF881.1.

[4] W. D. Rummler, "Two pulse spectral measurements.," Bell Telephone Labs, Whippany, NJ, USA, Technical Memorandum, MM-68-4121-15, 1968, p. 20.

[5] T. Berger and H. L. Groginsky, "Estimation of the spectral moments of pulse trains," presented at the International Conference on Information Theory (Tel Aviv, Israel), 1973, p. 9.

[6] K. Miller and M. Rochwarger, "A covariance approach to spectral moment estimation," *IEEE Transactions on Information Theory*, vol. 18, no. 5, pp. 588–596, 1972. DOI: 10.1109/TIT.1972.1054886.

[7] D. S. Zrnic, "Spectral moment estimates from correlated pulse pairs," *IEEE Transactions on Aerospace and Electronic Systems*, vol. AES-13, no. 4, pp. 344–354, 1977. DOI: 10.1109/TAES.1977.308467.

[8] R. E. Passarelli and A. D. Siggia, "The autocorrelation function and doppler spectral moments: Geometric and Asymptotic Interpretations," *Journal of Applied Meteorology and Climatology*, vol. 22, no. 10, pp. 1776–1787, 1983. DOI: 10.1175/1520-0450(1983)022⟨1776:TAFADS⟩2.0.CO;2.

[9] K. Miller and M. Rochwarger, "On estimating spectral moments in the presence of colored noise," *IEEE Transactions on Information Theory*, vol. 16, no. 3, pp. 303–309, 1970. DOI: 10.1109/TIT.1970.1054460.

[10] R. G. Strauch, R. A. Kropfli, W. B. Sweezy, W. R. Moninger, and R. W. Lee, "Improved Doppler velocity estimates by the poly-pulse-pair method," in *18th Conference on Radar Meteorology*, Jan. 1978, pp. 376–380.

[11] R. C. Srivastava, A. R. Jameson, and P. H. Hildebrand, "Time-domain computation of mean and variance of doppler spectra," *Journal of Applied Meteorology and Climatology*, vol. 18, no. 2, pp. 189–194, 1979. DOI: 10.1175/1520-0450(1979)018⟨0189:TDCOMA⟩2.0.CO;2.

[12] D. S. Zrnic, "Estimation of spectral moments for weather echoes," *IEEE Transactions on Geoscience Electronics*, vol. 17, no. 4, pp. 113–128, 1979. DOI: 10.1109/TGE.1979.294638.

[13] V. M. Melnikov and D. S. Zrnić, "Autocorrelation and cross-correlation estimators of polarimetric variables," *Journal of Atmospheric and Oceanic Technology*, vol. 24, no. 8, pp. 1337–1350, 2007. DOI: 10.1175/JTECH2054.1.

[14] L. Lei *et al.*, "Multilag correlation estimators for polarimetric radar measurements in the presence of noise," *Journal of Atmospheric and Oceanic Technology*, vol. 29, no. 6, pp. 772–795, 2012. DOI: 10.1175/JTECH-D-11-00010.1.

[15] D. Schvartzman, S. M. Torres, and D. Warde, "The Hybrid-Scan Estimators: Exploiting WSR-88D Split Cuts to Improve the Quality of Polarimetric-Variable Estimates," *Journal of Atmospheric and Oceanic Technology*, vol. 37, no. 2, pp. 299–315, 2020. DOI: 10.1175/JTECH-D-19-0071.1.

[16] S. Shao, K. Zhao, H. Chen, J. Chen, and H. Huang, "Validation of a multilag estimator on nju-cpol and a hybrid approach for improving polarimetric radar data quality," *Remote Sensing*, vol. 12, no. 1, 2020. DOI: 10.3390/rs12010180.

[17] D. Warde and D. Schvartzman, "Improved meteorological estimates for polarimetric weather radars using hybrid estimators," presented at the AMS 37th Conference on Environmental Information Processing Technologies (EIPT), American Meteorological Society, 2021, p. 14.

[18] I. R. Ivić, C. Curtis, and S. M. Torres, "Radial-based noise power estimation for weather radars," *Journal of Atmospheric and Oceanic Technology*, vol. 30, no. 12, pp. 2737–2753, 2013. DOI: 10.1175/JTECH-D-13-00008.1.

[19] L. H. Janssen and G. A. van der Spek, "The shape of doppler spectra from precipitation," *IEEE Transactions on Aerospace and Electronic Systems*, vol. AES-21, no. 2, pp. 208–219, 1985. DOI: 10.1109/TAES.1985.310618.

[20] R. Reinoso-Rondinel, T.-Y. Yu, and R. D. Palmer, "Investigation of doppler spectra from a tornadic supercell thunderstorm: Are they gaussian?," presented at the 33rd Conference on Radar Meteorology (Cairns, Australia, Aug. 6–10, 2007), Bureau of Meteorology Research Centre (BMRC), 2007, p. 8.

[21] T.-Y. Yu, R. R. Rondinel, and R. D. Palmer, "Investigation of non-gaussian doppler spectra observed by weather radar in a tornadic supercell," *Journal of Atmospheric and Oceanic Technology*, vol. 26, no. 3, pp. 444–461, 2009. DOI: 10.1175/2008JTECHA1124.1.

[22] R. E. Passarelli, "Parametric estimation of doppler spectral moments: An alternative ground clutter rejection technique," *Journal of Applied Meteorology and Climatology*, vol. 22, no. 5, pp. 850–857, 1983. DOI: 10.1175/1520-0450(1983)022⟨0850:PEODSM⟩2.0.CO;2.

[23] D. A. Warde and S. M. Torres, "Automatic detection and removal of ground clutter contamination on weather radars," presented at the 34rd Confrerence on Radar Meteorology (Williamsburg, VA, Oct. 5–9, 2009), American Meteorological Society, 2009, p. 10.

[24] S. M. Torres and D. A. Warde, “Ground clutter mitigation for weather radars using the autocorrelation spectral density,” *Journal of Atmospheric and Oceanic Technology*, vol. 31, no. 10, pp. 2049–2066, 2014. DOI: 10.1175/JTECH-D-13-00117.1.
[25] D. A. Warde and S. M. Torres, “Staggered-prt sequences for doppler weather radars. part ii: Ground clutter mitigation on the nexrad network using the clean-ap filter,” *Journal of Atmospheric and Oceanic Technology*, vol. 34, no. 3, pp. 703–716, 2017. DOI: 10.1175/JTECH-D-16-0072.1.
[26] Q. Cao, G. Zhang, R. D. Palmer, M. Knight, R. May, and R. J. Stafford, “Spectrum-time estimation and processing (step) for improving weather radar data quality,” *IEEE Transactions on Geoscience and Remote Sensing*, vol. 50, no. 11, pp. 4670–4683, 2012. DOI: 10.1109/TGRS.2012.2190608.
[27] T.-Y. Yu, Y. Wang, A. Shapiro, M. B. Yeary, D. S. Zrnić, and R. J. Doviak, “Characterization of tornado spectral signatures using higher-order spectra,” *Journal of Atmospheric and Oceanic Technology*, vol. 24, no. 12, pp. 1997–2013, 2007. DOI: 10.1175/2007JTECHA934.1.
[28] R. W. Lee, “Performance of the poly-pulse-pair doppler estimator,” Lassen Research, Memo 78-03, 1978.
[29] G. Meymaris, J. Williams, and J. Hubbert, “Performance of a proposed hybrid spectrum width estimator for the NEXRAD ORDA,” presented at the AMS 25th Conference on Interactive Information Processing Systems (IIPS) (Phoenix, AZ, USA), American Meteorological Society, 2009, p. 9.
[30] R. J. Doviak and D. S. Zrnić, *Doppler Radar and Weather Observations, 2nd ed.* San Diego: Academic Press, 1993.
[31] V. Bringi and V. Chandrasekar, *Polarimetric Doppler weather radar: principles and applications*. Cambridge university press, 2001.
[32] J. P. Pascual, J. Cogo, A. C. Rosell, and J. Areta, “Multipulse processing algorithm for improving mean velocity estimation in weather radar,” *IEEE Transactions on Geoscience and Remote Sensing*, vol. 60, pp. 1–10, 2022. DOI: 10.1109/TGRS.2021.3066810.
[33] J.-S. Lee, K. Hoppel, S. Mango, and A. Miller, “Intensity and phase statistics of multilook polarimetric and interferometric sar imagery,” *IEEE Transactions on Geoscience and Remote Sensing*, vol. 32, no. 5, pp. 1017–1028, 1994. DOI: 10.1109/36.312890.
[34] D. S. Zrnić, “Simulation of weatherlike doppler spectra and signals,” *Journal of Applied Meteorology and Climatology*, vol. 14, no. 4, pp. 619–620, 1975. DOI: 10.1175/1520-0450(1975)014⟨0619:SOWDSA⟩2.0.CO;2.
[35] C. D. Curtis, “Weather radar time series simulation: Improving accuracy and performance,” *Journal of Atmospheric and Oceanic Technology*, vol. 35, no. 11, pp. 2169–2187, 2018. DOI: 10.1175/JTECH-D-17-0215.1.
[36] D. Schvartzman and C. D. Curtis, “Signal processing and radar characteristics (sparc) simulator: A flexible dual-polarization weather-radar signal simulation framework based on preexisting radar-variable data,” *IEEE Journal of Selected Topics in Applied Earth Observations and Remote Sensing*, vol. 12, no. 1, pp. 135–150, 2019. DOI: 10.1109/JSTARS.2018.2885614.
[37] G. Zhang, *Weather Radar Polarimetry*, 1st. USA: CRC Press, Inc., 2016.
[38] M. R. Kumjian, “Principles and applications of dual-polarization weather radar. Part I: Description of the Polarimetric Radar Variables,” 19, vol. 1, National Weather Association, 2013, pp. 226–242.
[39] D. Warde and S. Torres, “Improved spectrum width estimators for doppler weather radars,” presented at the 8th European Conference on Radar in Meteorology and Hydrology (Garmisch-Partenkirchen, Germany, Sep. 1–5, 2014), Deutscher Wetterdienst (DWD) and Deutsches Zentrum für Luft- und Raumfahrt (DLR), 2014, p. 8.
[40] D. A. Warde and S. M. Torres, “Spectrum Width Estimation Using Matched Autocorrelations,” *IEEE Geoscience and Remote Sensing Letters*, vol. 14, no. 10, pp. 1661–1664, 2017. DOI: 10.1109/LGRS.2017.2726898.
[41] M. Reed and B. Simon, *Methods of Modern Mathematical Physics, I: Functional analysis*. San Diego, CA: Academic Press, 1980.

Appendix

We provide the following derivations using the perturbation analysis, for those readers interested in pursuing a theoretical analysis of the proposed GMLE presented. Perturbation analysis is used to describe the statistical errors associated with different estimators used in weather radar signal processing ([12, 13, 30, 31, 37]) and [12, 30] give limitations on its use. The basic premise is that the errors associated with the estimator are small (assumed Gaussian) and a truncated Taylor expansion is used to evaluate the bias and standard deviation of the estimator.

Using multiple index notation [41] for the set of $Y_X = \exp(y_X)$ $[Z_W = \exp(z_W)]$ used in the estimator $\hat{T} : \mathbb{R}^x \to \mathbb{R}$ $\left(\hat{S} : \mathbb{R}^w \to \mathbb{R}\right)$, $\Big(y_X, \hat{y}_X \in \mathbb{R}^x$ $(z_W, \hat{z}_W \in \mathbb{R}^w)$; with $n \in \mathbb{N}_0$; and $\alpha, \beta \in \mathbb{N}_0^x$; $|\alpha| = \alpha_1 + \alpha_2 + \cdots + \alpha_x$; $(|\beta| = \beta_1 + \beta_2 + \cdots + \beta_w)$; $\alpha! = \alpha_1! \cdot \alpha_2! \cdots \alpha_x!$ $(\beta! = \beta_1! \cdot \beta_2! \cdots \beta_w!)$, we can express

$$
\begin{aligned}
\hat{T}\left(\Delta\hat{Y}_X\right) &= \sum_{|\alpha|\leq n} \frac{\partial^\alpha \hat{T}\left(\Delta\hat{Y}_X\right)}{\alpha!}\left(\Delta\hat{Y}_X\right)^\alpha + R_n\left(\Delta\hat{Y}_X\right) \\
\hat{S}\left(\Delta\hat{Z}_W\right) &= \sum_{|\beta|\leq n} \frac{\partial^\beta \hat{S}\left(\Delta\hat{Z}_W\right)}{\beta!}\left(\Delta\hat{Z}_W\right)^\beta + R_n\left(\Delta\hat{Z}_W\right)
\end{aligned}
\tag{32}
$$

where $\Delta\hat{Y}_X = \hat{Y}_X - Y_X$, $\Delta\hat{Z}_W = \hat{Z}_W - Z_W$, R_n is the remainder. Extracting the first term in $\hat{T}$ $\left(\hat{S}\right)$ and choosing n large enough to make the remainder insignificant, the perturbations (difference between the estimator and the true value) is approximated as,

$$
\begin{aligned}
\delta\hat{T}\left(\Delta\hat{Y}\right) = \hat{T}\left(\hat{Y}_X\right) - T\left(Y_X\right) &\approx \sum_{\substack{|\alpha| \leqslant n \\ |\alpha| \neq 0}} \frac{\partial^\alpha \hat{T}\left(\Delta\hat{Y}_X\right)}{\alpha!}\left(\Delta\hat{Y}_X\right)^\alpha \\
\delta\hat{S}\left(\Delta\hat{Z}_W\right) = \hat{S}\left(\hat{Z}_W\right) - S\left(Z_W\right) &\approx \sum_{\substack{|\beta| \leqslant n \\ |\beta| \neq 0}} \frac{\partial^\beta \hat{S}\left(\Delta\hat{Z}_W\right)}{\beta!}\left(\Delta\hat{Z}_W\right)^\beta
\end{aligned}
\tag{33}
$$

Then, the bias B and variance V are calculated as the ensemble average of the perturbations,

$$
\begin{aligned}
B\left[\hat{T}\right] = \left\langle \delta\hat{T} \right\rangle \text{ and } V\left[\hat{T}\right] = \left\langle \left[\delta\hat{T}\right]^2 \right\rangle \text{ and} \\
B\left[\hat{S}\right] = \left\langle \delta\hat{S} \right\rangle \text{ and } V\left[\hat{S}\right] = \left\langle \left[\delta\hat{S}\right]^2 \right\rangle
\end{aligned}
\tag{34}
$$

David Warde (Senior Member, IEEE) received the B.S. degree (dual major) in computer science and management/computer information systems from Park University, Parkview, MO, USA, in 2004 and the Electronic/Instrument Technology A.S. degree from Excelsior College, Albany, NY, USA, in 1997. From 1982 to 2002, he served as an Aviation Electronics Technician with the U.S. Navy retiring ATCS (AW/NAC). From 2003 to 2008, he worked as Radar Systems Engineer support contractor for the WSR-88D Radar Operations Center, where he designed hardware upgrades to the WSR-88D test beds and provided support of signal processing enhancements to the operational system including the base moment estimators, spectral ground clutter filter, and automated ground clutter detection. In 2008, he joined the Cooperative Institute for Severe and High-Impact Weather Research and Operations (CIWRO), formerly known as the Cooperative Institute for Mesoscale Meteorological Studies (CIMMS), at The University of Oklahoma, Norman, OK, USA, where he currently is a Research Associate affiliated with the National Severe Storms Laboratory (NSSL). As a member of the Advanced Radar Techniques group, he conducts research and development of innovative signal processing and adaptive sensing techniques to improve the quality, coverage, accuracy, and timeliness of meteorological products from weather radars. In addition, he is involved in the exploration and demonstration of unique capabilities offered by phased array radar for weather observations; and the transfer of technology to existing radar systems in government, public, and private organizations. Mr. Warde has received numerous awards throughout his career. Most recently, he received the 2011 Department of Commence Gold Medal as a member of the Radar Research and Development Division at NSSL for scientific and engineering excellence in adapting military phased array radar technology to improve U.S. weather radar capabilities.

David Schvartzman (Senior Member, IEEE) was born in Piracicaba, SP, Brazil, on March 17, 1988. He received the B.S. degree in electrical and computer engineering from the National University of Asunción, San Lorenzo, Paraguay, in 2011, and the M.S. and Ph.D. degrees in electrical and computer engineering from the University of Oklahoma, Norman, OK, USA, in 2015 and 2020, respectively. From 2015 to 2020, he was a Research Scientist with the NOAA National Severe Storms Laboratory (NSSL) and the Cooperative Institute for Severe and High-Impact Weather Research and Operations (CIWRO). From 2021 to mid-2022, he was a Research Scientist with the Advanced Radar Research Center (ARRC) at The University of Oklahoma. Currently, he is an Assistant Professor with the University of Oklahoma School of Meteorology, affiliated with the ARRC. He works on novel signal and array processing algorithms to improve understanding of atmospheric processes using phased array radar. He also works on calibration and integration of phased array radar systems.

Dr. Schvartzman is also an Adjunct Assistant Professor with the University of Oklahoma School of Electrical and Computer Engineering. He is the recipient of the 2023 IEEE R5 *Outstanding Young Professional* Award and the 2019 American Meteorological Society's *Spiros G. Geotis* Prize. He is a Senior Member of the Institute for Electrical and Electronic Engineers (IEEE) and a member of the American Meteorological Society (AMS).

Christopher D. Curtis received the B.S. degree in mathematics and the Ph.D. degree in engineering from the University of Oklahoma, Norman, in 1992 and 2009, respectively, and the M.S. degree in applied mathematics from the University of Illinois, Champaign-Urbana, in 1993. From 1995 to 1999, he was with the Radar Signal Processing Group at Texas Instruments and later Raytheon in Plano, TX. He is currently a research scientist with the Cooperative Institute for Severe and High-Impact Weather Research and Operations (CIWRO), University of Oklahoma, which is affiliated with the National Severe Storms Laboratory (NSSL). He is a member of the Advanced Radar Techniques team in NSSL's Radar Research and Development Division. His research interests are in the area of signal processing with applications to phased array and Doppler weather radars, including range oversampling processing, adaptive beamforming, radar variable estimation, and radar interference.

Dr. Curtis is a member of Phi Beta Kappa.